Research Open

Geology, Earth and Marine Sciences
Volume 8 Issue 5

Research Article

Diamond in Pycnite-Rock from Altenberg and in the Topaz from the Famous Schneckenstein Deposit

Rainer Thomas*

Im Waldwinkel 8, D-14662 Friesack, Germany

Corresponding author: Rainer Thomas, Im Waldwinkel 8, D-14662 Friesack, Germany

Received: May 26, 2026; **Accepted:** May 30, 2026; **Published:** June 02, 2026

Abstract

This study investigates topaz from Altenberg pycnite rock and the Schneckenstein deposit, with emphasis on fluorine variability and the occurrence of carbon phases. Raman spectroscopy was used to characterize topaz, determine fluorine contents, and identify inclusions. The results show that Altenberg pycnite is compositionally heterogeneous, containing both fluorine-rich and fluorine-poorer domains, whereas Schneckenstein topaz is associated with unusual Ti-rich topaz-rutile inclusions and small spheres of diamond-like carbon and diamond. The discovery of diamond and related carbon phases in both occurrences is interpreted as evidence that supercritical fluids and/or deeper melts participated in the formation of these rocks and minerals.

Keywords: *Topaz, Pycnite, Altenberg, Schneckenstein, Raman spectroscopy, Fluorine, Diamond, Diamond-like carbon, Supercritical fluids, Mineral inclusions*

Introduction

Topaz [$Al_2SiO_4F_x(OH)_{2-x}$], normally an orthorhombic F-rich mineral, is of mineralogical and genetic interest. The F-content is up to 20.65% F, and x=1.4-2.0. If we speak in%, we mean always [%(g/g)], because wt% is not a permitted unit since 1988 [1]. First, we will present some simple mineralogical characteristics. The F-content and the lattice angle 2V characterize mainly the topaz. Table 1 presents topaz data from a selection of crystals [2-4].

Generally, topaz is orthorhombic and has 2V axis angles of 50-68°. Especially the pycnite from Altenberg is a little bit unusual. The c-axis of the topaz crystals makes an angle of about 12° with the a-b plane. Using conoscopic mode on a fine-grained fraction of topaz/pycnite cleavage lamellae reveals optical biaxial symmetry. However, that is not clear proof because many grains show unclear two axes, unlike the Schneckenstein topaz. In the same riddle fraction from Schneckenstein, most crystals show a clear biaxial behavior.

Table 1: Results of the X-ray determination of fluorine in topaz according to Thomas (1979 and 1982) [2-3] using the Ribbe and Rosenberg (1971) [5] method. The (200) peak of NaCl is the reference. $\Delta_{(021)}=2\Theta_{NaCl\ 200} - 2\Theta_{Topaz\ 021}$, the optical 2V-determination, and the Raman determination using equation (1) presented by Loges et al. 2025 [6].

Thomas (1979 and 1982) [2,3]					According to Loges et al. 2025, Equ. (1)	
Sample	**$\Delta_{(021)}$**	**F [%(g/g)]**	**n**	**2V [°]**	**F [%(g/g)]**	n
San Luis Potosí, Mexico	3.909 ± 0.006	16.05 ± 0.21	23	50.6 ± 0.9	16.79 ± 0.35	11
Ehrenfriedersdorf, Sauberg mine: Top-5	3.845 ± 0.004	18.33 ± 0.14	7	60.1 ± 0.9	19.08 ± 0.35	10
Ehrenfriedersdorf, Sauberg mine: Top-4	3.839 ± 0.005	18.55 ± 0.18	8	61.0 ± 0.8	19.54 ± 0.35	10
Ehrenfriedersdorf, Sauberg mine: Top-2	3.825 ± 0.004	19.05 ± 0.14	11	63.1 ± 0.6	19.02 ± 0.23	11
Schneckenstein	3.822 ± 0.004	19.15 ± 0.14	11	63.5 ± 0.6	19.26 ± 0.74	10
Altenberg pycnite II	3.811 ± 0.005	19.55 ± 0.18	13	65.2 ± 0.8	19.44 ± 0.45	8
Zinnwald pycnite	3.814 ± 0.005	19.44 ± 0.18	9	64.7 ± 0.8	19.94 ± 0.68	10
Amerika bei Penig, Saxonia	3.811 ± 0.009	19.55 ± 0.32	9	65.2 ± 1.4	n.b.	-
Otani Jama, Japan	3.805 ± 0.005	19.76 ± 0.18	8	66.0 ± 0.8	n.b.	-
Altenberg, pycnite I	3.803 ± 0.005	19.83 ± 0.18	15	66.3 ± 0.8	n.b.	-
Ouro Preto, Brazil	3.802 ± 0.003	19.87 ± 0.11	10	66.5 ± 0.4	20.00 ± 0.45	
Sadisdorf, pycnite	3.801 ± 0.007	19.90 ± 0.25	7	66.6 ± 1.0	19.98 ± 0.40	18
Topaz Mountain, Thomas Range, Utah, USA	3.800 ± 0.003	19.94 ± 0.11	10	66.8 ± 0.5	20.11 ± 1.00	14
Spitzkopje, Namibia	3.796 ± 0.007	20.08 ± 0.25	9	67.4 ± 1.0	20.19 ± 0.59	22
Tröstau, Fichtelgebirge	3.796 ± 0.006	20.08 ± 0.21	7	67.4 ± 0.9	n.b.	-
Epprechtstein, Fichtelgebirge	3.795 ± 0.008	20.12 ± 0.29	10	67.5 ± 1.2	20.14 ± 0.14	10

Note that in the original table (Thomas, 1979 and 1982) [2,3], the names of the topazes from San Luis Potosí, Mexico, and Ouro Preto, Brazil, are mixed up.
n.b. – means the samples are not present anymore.

According to Gatta et al. (2006) [7], topaz is the stable phase above 12 GPa and 1100°C. The Raman spectroscopic determination of F according to Loges et al. (2025) [6] and Thomas (2026a) [4] showed that the Altenberg topaz contain an relative high portion of topaz with lower fluorine content: F=15.66 ± 2.01% (n =11). Similar lower results were obtained for the black topaz inclusions in normal Topaz from Schneckenstein/W-Erzgebirge: F=16.52 ± 0.76% (n=10). However, we do not want to repeat the results reported in Thomas (2026a) [4] but rather present completely new results. That concerns the topaz and the not-so-rare diamond inclusions. The diamond is, of course, a little bit different from a perfect diamond because, on the long journey from the place of origin to the place of deposition via supercritical fluid (SCF), it undergoes extreme thermal and pressure stress. The spectren look, in a sense, like nanodiamonds.

Methods and Samples

Raman Spectroscopy

We used the Raman spectroscopy to identify the topaz-specific Raman bands and determine the fluorine concentration according to Loges et al. (2025) [6] and Thomas (2026a) [4]. Furthermore, Raman spectroscopy was very helpful in distinguishing the Ti-rich topaz from the wine-yellow Schneckenstein topaz. Another task is to provide clear proof of diamond and DLC (diamond-like carbon) in topaz from Altenberg and Scheckenstein. According to Zaitsev (2001) [8], the more correct term is "diamond-like materials." The data presented here were acquired using an EnSpectr Raman microscope (RamMics R532). Measurements covered the spectral range from 0 to 4000 cm^{-1} and were conducted with a single-mode 532 nm laser operating at a maximum output of 50 mW. Analytical settings included a 20 µm entrance aperture, a holographic grating of 1800 g mm^{-1}, and a spectral resolution of approximately 4 cm^{-1} (generally for the whole range). For most analyses of different topaz crystals, a long-working-distance Olympus LMPlanFL 100× objective was used. Using lower magnifications introduces the problem of excitation of different F-bearing areas within the topaz crystal (lamellas). Laser power at the sample surface was continuously adjustable down to 0.02 mW. Higher powers (up to 50 mW) were applied only for overview measurements. Generally, for F-concentration measurements, we used 0.9 mW on the sample in the range from 75 to 900 cm^{-1} to prevent local heating. For the measurement of the OH band of topaz, the 0-4000 cm^{-1} range was used (which is not, however, the object of the present study). For OH-rich topazes transported via supercritical fluids, we have determined an X_{OH}=0.83 ± 0.08 (at another place). Raman band positions were calibrated before and after each measurement series using the Si band of a semiconductor-grade single-crystal silicon chip. Based on 20 repeated measurements, run-to-run reproducibility was ± 0.2 cm^{-1} for silicon (520.2 ± 0.2 cm^{-1}) in the measuring range 75 to 900 cm^{-1}.

Fluorine Determination

The Raman method for fluorite determination is described in detail by Thomas (2026a) [4] and is based on the method of Loges et al. (2025) [6].

Samples

A detailed description of the localities of the topaz crystals used is in both books: Topas (1997) [9] and the licensed edition topaz (2011) – [10]. A comprehensive description of the pycnite-bearing rock, including analyses, from Altenberg/E-Erzgebirge, Germany, is provided by Recknagel (1969), Weinhold (2002) [11], and Lausch (2024) [12]. For the preparation of the Altenberg samples, diamond was never used; for polishing, an alumina suspension (50 nm, pH 7-8, 200 g/l) was used. The topaz from the Schneckenstein dates from a visit to the Schneckenstein in October 1960, together with Peter Haupt. In the study, only centimeter-sized natural crystal cleavages perpendicular to the c-axis are generally used (Figure 1). A description of the occurrence of the "Schneckenstein" is given in Lahl (2012) [13].

Results

New Results on Topaz (Pycnite) from Altenberg

The pycnite variety of topaz is not uniform in its F content. The main part has a F-concentration of 19.55 ± 0.18% (n=13), whereas in a smaller part the concentration is lower: F=15.66 ± 2.01% (n=11). By the mixture, the cleavage is not uniform. A 12° "inclination of the c-axis against the a–b plane" is a big red flag that what we are seeing is not a change from orthorhombic → monoclinic topaz, but rather an orientation/domain effect (misindexing, twinning, or internal lattice bending/mosaicity). However, as we will see, the high-pressure modifications (monocline system) are not absolutely impossible. However, the pressure should exceed 24 GPa. Another important new finding is the proof of diamond or DLC (diamond-like carbon).

New Results on Topaz from Schneckenstein

Normally, the topaz from Schneckenstein is yellow, water-clear, and contains only a small number of solid mineral inclusions (besides many fluid inclusions, which often contain sassolite daughter phases (see Gilg and Thomas in: Topaz, 2011) [10]. Later, we will see that the fluid inclusions are, as a rule, secondary, and that the F-concentration-

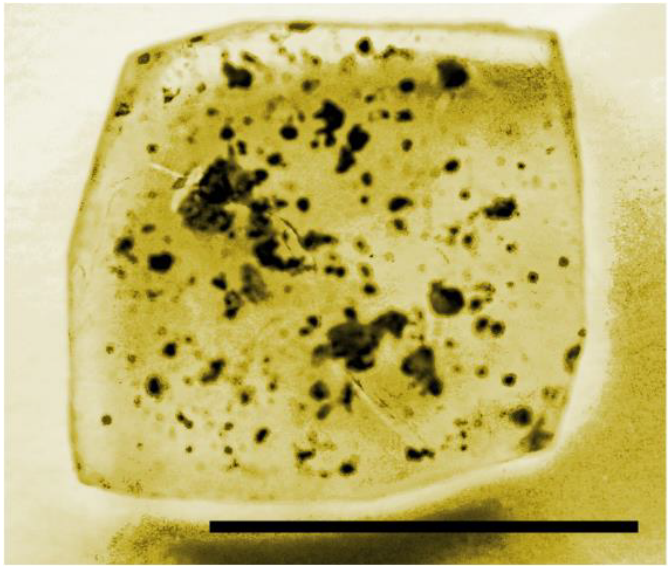

Figure 1: Topaz crystal cleavage with Ti-rich topaz and DLC inclusions. The scale is 1 cm.

temperature diagram (Figure 7 in Thomas 2026a) [4] has only a limited meaning. During the study of samples collected in 1960, we found that, in addition to black spherical topaz-like aggregates (which contain some graphite), topaz also contains small brown-orange spheres, which are topaz with significantly lower F-content. Striking inclusions in topaz (Figure 2) are composed of rutile and topaz; the relative amount of rutile in these inclusions is similar. So, the composition of this inclusion type is ± the same, suggesting a homogeneous formation. That means that this inclusion was at high temperature and high pressure, a single homogeneous mineral phase – in our case, a Ti-rich topaz, in analogy to the Ge- and Ga-rich analog of topaz, the krieselite (Spivak et al., 2021 [14] and Setkova et al., 2024) [15]. A further large surprise was the finding of small spheres (up to 10 µm in diameter) of diamond and DLC in the topaz host, as well as DLC in the old topaz-rutile inclusions in the same host. The finding of diamond spheres in both topaz types (pycnite from Altenberg, topaz from Schneckenstein) demonstrates that during the formation of the rock (pycnite-rock, topaz breccia), supercritical fluids (SCF) and/or supercritical melts (SCM) participated more or less strongly in the formation.

Such quite unusual inclusions, if present, always have the same bulk composition. Of course, that is strictly speaking speculative; however, it looks like so. The substitution of Al by Ti^{4}+ ions in the octahedral position is conceivable and, under HT and HP, realistic. The availability of titan is also important. There are well-formed topaz crystals that are very rich in ilmenite. Rutile and anatase are rare minerals and are (in the case of rutile) mostly arranged as a single small crystal in topaz. Anatase is absent in the matrix. The appearance of rutile and anatase clusters within topaz inclusions is remarkable. Figures 3 and 4 show examples of Raman spectra of the Ti-phases.

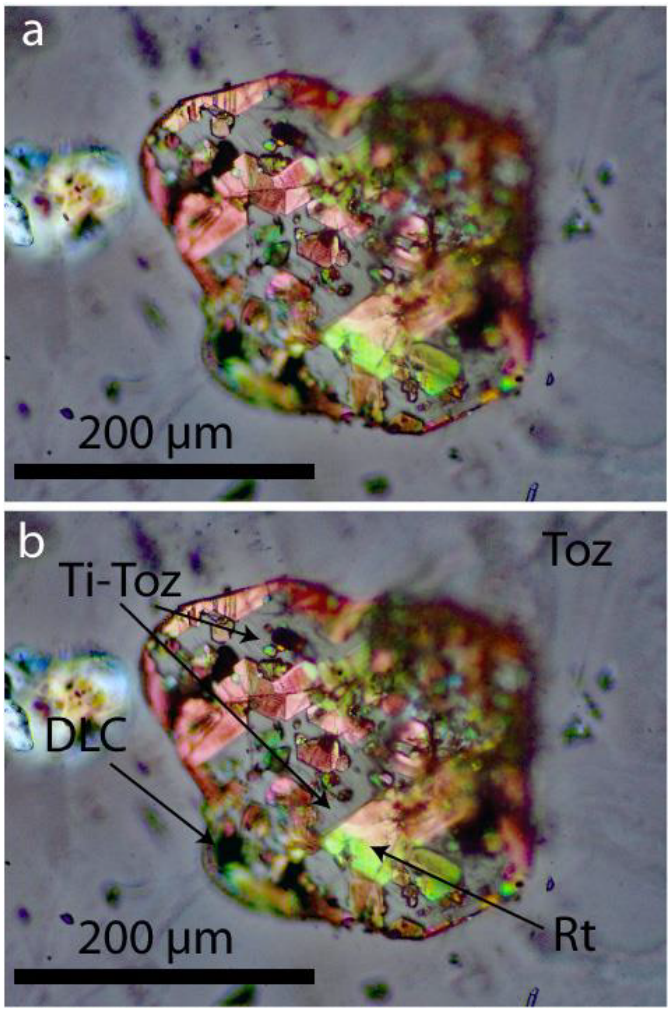

Figure 2: Inclusion in topaz (Toz) from Schneckenstein. The red and green minerals are mostly rutile, with a little anatase, and the grey parts are Ti-rich topaz (Ti-Toz). And the black crystals are DLC (diamond-like carbon).

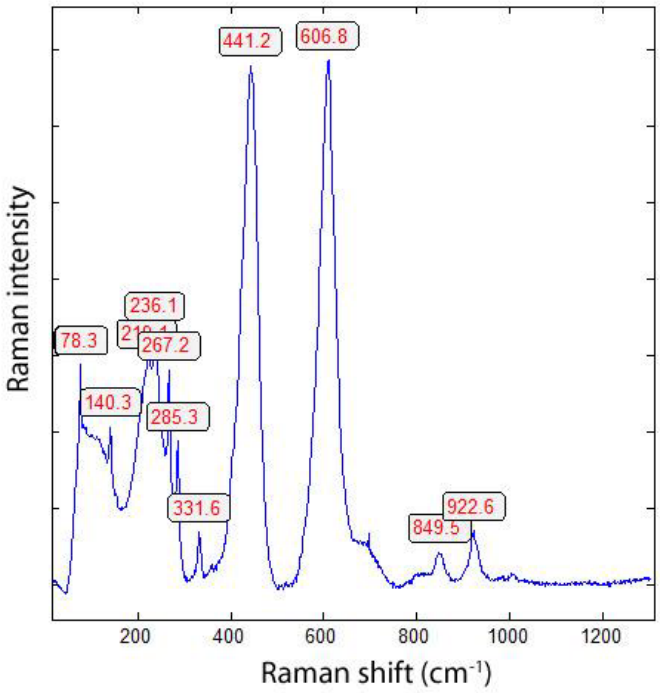

Figure 3: Raman spectrum of rutile in the inclusion (Figure 2, green crystal).

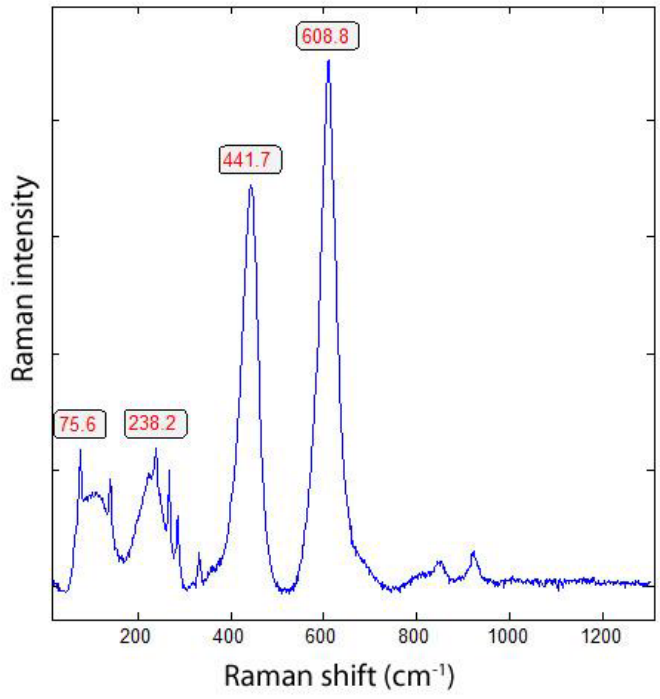

Figure 4: Raman spectrum of rutile in the inclusion (Figure 2, red crystal).

Figures 3 and 4 show the Raman spectra of rutile in the topaz inclusion in the matrix topaz crystal. Both spectra show remnants of TiO_2-II [16], which means that rutile and TiO_2-II coexisted at HP and HT (Figure 5). The black crystals in Figure 6 are DLC (diamond-like carbon) in the rutile-bearing topaz inclusion in topaz from Schneckenstein.

The discovery of diamond-like carbon in the rutile-topaz inclusion in water-clear topaz prompted an intense search for diamonds in both studied topaz types. At first, we found diamond and DLC in pycnite-topaz quartz from Altenberg (Figure 6, and further down in Figure 8b).

Table 2 presents the Raman results for diamond and DLC in both samples (pycnite quartz, pycnite from Altenberg, and topaz from Schneckenstein.

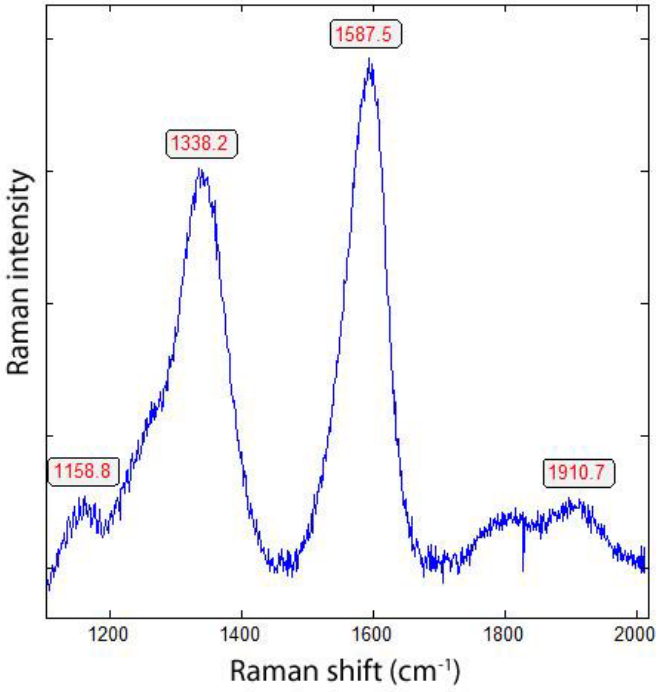

Figure 5: Raman spectrum of diamond-like carbon (DLC) in Figure 2.

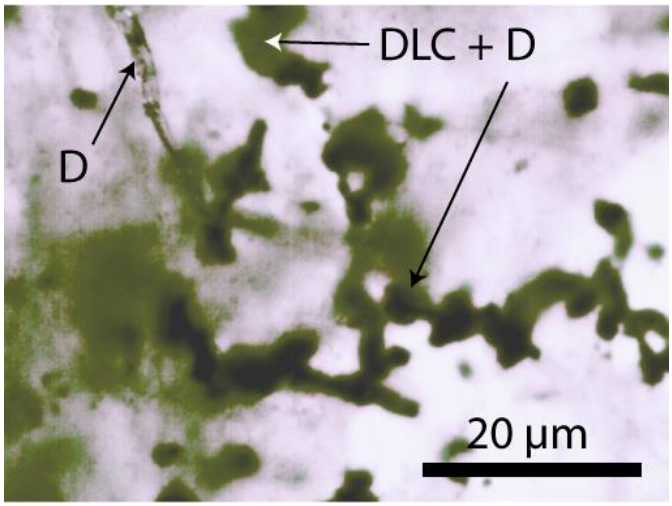

Figure 6: DLC and diamond in pycnite-topaz from Altenberg.

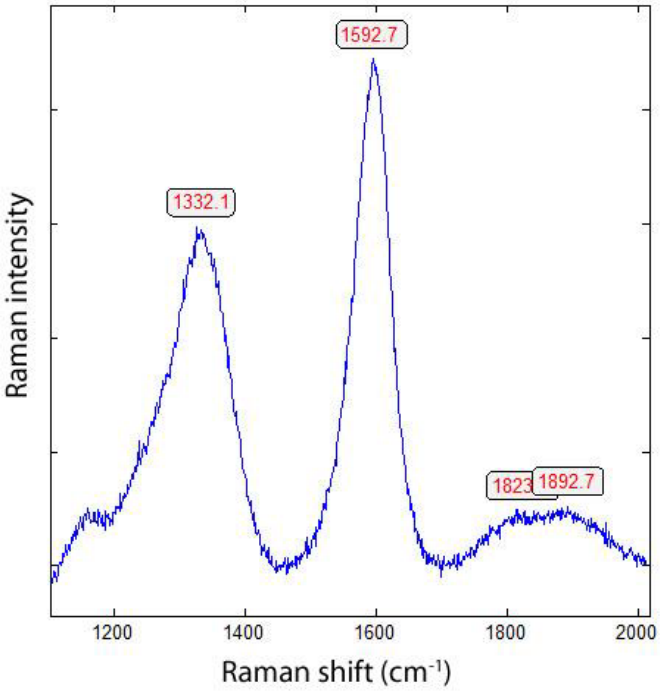

Figure 7: Raman spectrum of diamond in pycnite-topaz from Altenberg (see Figure 6).

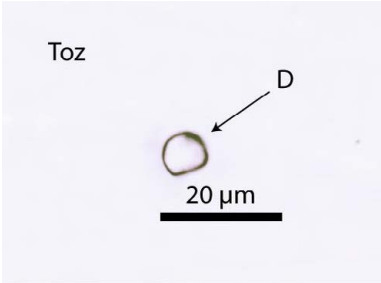

Figure 8a: Water-clear diamond (D) sphere in topaz (Toz) from Schneckenstein. The Raman spectrum is in Figure 8b.

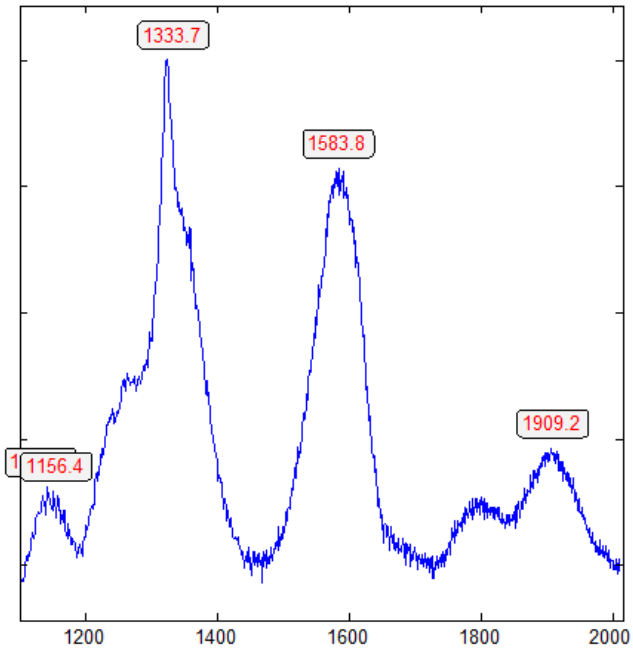

Figure 8b: Typical first-order Raman spectrum of diamond in topaz from Schneckenstein.

Table 2: Results of the Raman measurement in the first-order range of diamond.

Diamond, DLC	FWHM	G-band	FWHM	n
Quartz from Altenberg (Thomas, 2025) [17]				
1324.2 ± 10.2 cm^{-1}	74.8 ± 18.0 cm^{-1}	1585.8 ± 7.6 cm^{-1}	57.0 ± 7.8 cm^{-1}	18
Topaz (Pycnite) from Altenberg				
1330.2 ± 2.2 cm^{-1}	74.6 ± 21.4 cm^{-1}	1574.7 ± 9.4 cm^{-1}	64.3 ± 15.5 cm^{-1}	13
1339.0 ± 3.6 cm^{-1}	79.3 ± 6.0 cm^{-1}	1593.3 ± 14.7 cm^{-1}	64.9 ± 15.6 cm^{-1}	12
Topaz from Schneckenstein				
1326.6 ± 4.2 cm^{-1}	41.6 ± 25.4 cm^{-1}	1597.3 ± 2.8 cm^{-1}	61.2 ± 3.5 cm^{-1}	14
1304.2 ± 1.9 cm^{-1}	22.7 ± 1.7 cm^{-1}	n.d.	n.d.	7

DLC – Diamond-like carbon, FWHM – Full Width at Half Maximum. n – number of measured crystals. n.d. – not detected.

Note: The intensity of the second and third-order Raman bands (e.g., the 2666 cm^{-1} and the 3825 cm^{-1} peaks) of diamond is very weak and has a large FWHM, and at 2664 cm^{-1}, the topaz from Schneckenstein shows a relatively strong Raman background of the (OH)-band in this region.

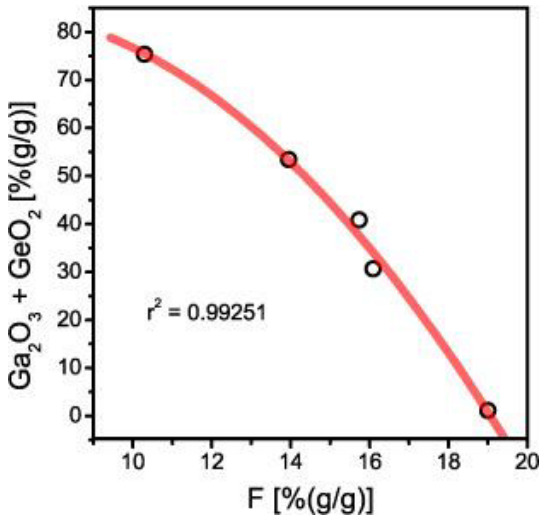

Figure 9: Sum of Ga_2O_3 and GeO_2 versus fluorine in Ga, Ge-rich topaz according to Setkova et al. (2024).

The discovery of diamond in topaz supports the idea of the formation of Ti-rich diamond, because the interaction of supercritical phases (SCF, SCM) from mantle depths can yield 5 GPa pressures exceeding. At the crustal level, with low HP and HT values, the Ti-topaz phase is clearly unstable. The rutile concentration in the Ti-rich topaz (Figure 2) looks very high. However, if we take the analyses given by Setkova et al. (2024) [15] for Ga- and Ge-rich topaz, we obtain the following relationship.

The pure Ge-substituted topaz analog is krieselite, with the formula $Al_2(GeO_4)F_2$, and the corresponding Ti-topaz analog is then $Al_2(TiO_4)F_2$. Besides the remnants of Ti-topaz analog, some topaz crystals contain black, spherical, or rounded crystals that also exhibit the topaz Raman spectrum (Figure 10).

The origin of the black color of the topaz is unclear. Possible materials are simple carbon, graphite, and DLC. More studies are necessary.

According to Beny and Piriou (1987) [18], all Raman lines are characteristic of topaz. Using long-time spectra in the narrow range

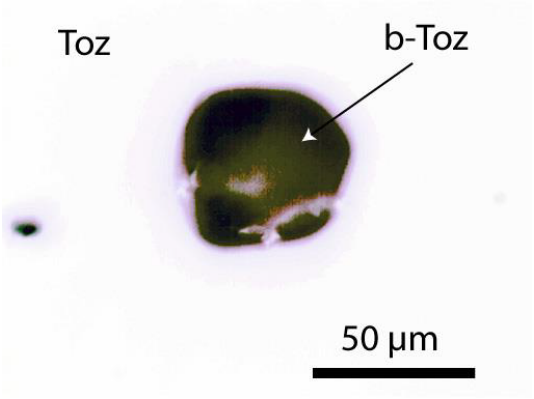

Figure 10a: Black topaz (b-Toz)) in matrix topaz (Toz) from Schneckenstein.

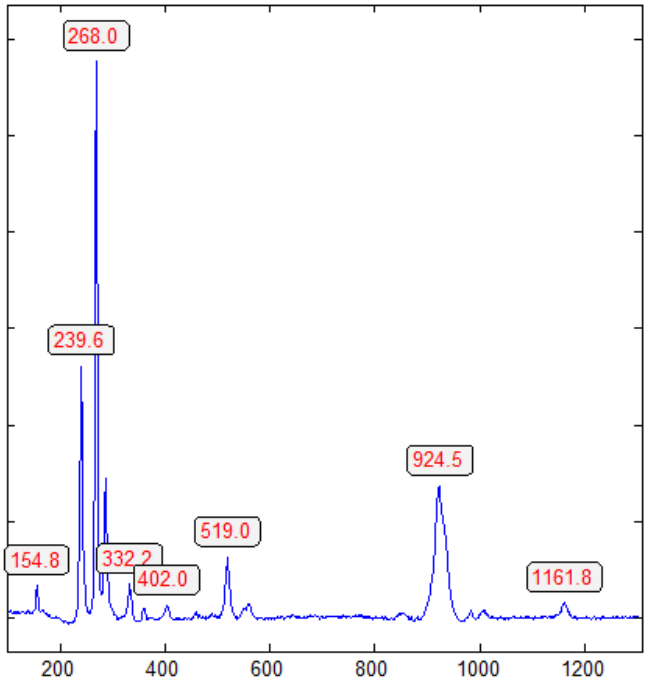

Figure 10b: Raman spectrum of a black topaz inclusion in topaz from Schneckenstein.

of 50 to 200 and 400 to 900 cm^{-1}, three Raman lines appear, which are characteristic of anatase (145, 514, and 638 cm^{-1}). Obviously, that black Ti-rich topaz is on the verge of disintegrating into anatase and topaz. Additionally, several "anomalous" secondary O-H stretching bands can be seen in the region from 3200 to 3950 cm^{-1} (see Beny and Piriou, 1987) [18]. The black coloring of the topaz is caused by DLC (see Figure 10c).

Interpretation

After the first proof of spherical diamonds in pycnite-topaz from Altenberg, we have found unusual rutile-(anatase)-rich topaz inclusions in topaz from Schneckenstein. The appearance of this type of inclusion suggests that the inclusion was primarily a homogeneous mineral phase – a very Ti-rich topaz. Because this inclusion is now present in the Schneckenstein topaz in the upper crust, we can assume that the primary homogeneous inclusion originated from greater depth. That is supported by the mostly spherical diamond crystals, which we interpret

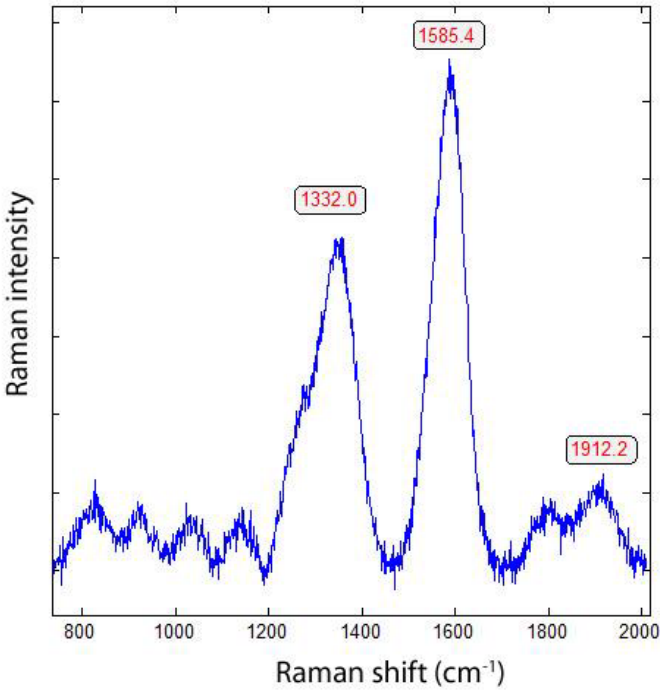

Figure 10c: Raman spectrum of black Ti-rich topaz in the first-order carbon range.

as evidence of the SCF and/or SCM originating from mantle depths [17,19]. This statement is supported by numerous studies over the past few years that have provided evidence of HP and HT minerals (cristobalite X-I, coesite, diamond, lonsdaleite, moissanite, orthorhombic cassiterite, stishovite, and others) in Variscan mineralization in the Lusatian Mts, the Saxon Granulite Mts., the Erzgebirge, Slavkovský les, and Thuringia [17, 19, 20-24]. At last, the ascent of SCF and SCM from the mantle into the crust is not a rare, insignificant event. Besides water and other volatiles (F, CO_2, CH_4, higher hydrocarbons), economic important elements like Sn (as orthorhombic cassiterite) and many others, as well as diamond, lonsdaleite, and moissanite, are evidence of the interaction between mantle and crust via SCF and SCM (e.g., Thomas and Rericha, 2025) [25-27]. Such phases from the mantle region must have left their traces not only as minerals but also in significant isotope shifts and trace element ratios.

Conclusions

In summary, Raman spectroscopy shows that topaz from Altenberg pycnite is compositionally heterogeneous and includes domains with distinctly lower fluorine contents, whereas topaz from Schneckenstein contains unusual Ti-rich topaz-rutile inclusions together with diamond-like carbon and diamond. The occurrence of these carbon phases in both localities, combined with evidence for high-pressure Ti-bearing inclusions, supports the interpretation that supercritical fluids and/or melts derived from greater depth contributed to the formation of the pycnite rock and Schneckenstein topaz. These results strengthen the view that mantle-derived components may have played a significant role in the evolution of Variscan mineralization in the Erzgebirge.

Acknowledgment

My interest in topaz began in October 1960 during a visit to the Schneckenstein crag with Peter Haupt, also an apprentice at the Zwickau coal mine, whose father participated in the drilling program by Prof. L. Baumann and S. Gorny.

References

1. Ebel HF, Bliefert C, Russey WE (2004) The Art if Scientific Writing. Wiley-VCH. Pg: 595.
2. Thomas R (1979) Untersuchungen von Einschlüssen zur thermodynamischen aund physikochemischen Charakteristic lagerstättenbildender Lösungen und Prozesse im magmatischen und postmagmatischen Bereich. Bergakademie Freiberg, Dissertation A. Pg: 245 + 83.
3. Thomas R (1982) Ergebnisse der thermobarometrischen Untersuchungen an Flüssigkeitseinschlüssen in Mineralen der postmagmatischen Zinn-wolfram-mineralisation des Erzgebirges. Freiberger Forschungshefte (FFH). C370: 5-85 + I-XVI.
4. Thomas R (2026a) Raman spectroscopic determination of fluorine in topaz. *Geol Earth Mar Sci* 8: 1-8.
5. Ribbe PH, Rosenberg PE (1971) Optical and X-ray determinative method for fluorine in topaz. *American Mineralogist* 56: 1812-1821.
6. Loges A, Qiao S, Zhong X, Fuller J, John T (2025) Determination of fluorine concentration in Topaz using Raman spectroscopy. *American Mineralogist* (Revision 2). Pg: 45.
7. Gatta GD, Nestola F, Bromiley GD, Loose A (2006) New insight into crystal chemistry of topaz: A multi-methodological study. *American Mineralogist* 91: 1839-1846.
8. Zaitsev AM (2001) Optical Properties of Diamond -A Data Handbook. Berlin, Heidelberg, New York, *Springer*. Pg: 502.
9. Topas – Das prachtvolle Mineral, der lebhafte Edelstein (1997). Extra Lapis No. 13. Christian Weise Verlag München. Pg: 95.
10. Topaz – Perfect Cleavage (2011). Licensed edition. Extra Lapis No. 14. Christian Weise Verlag München. Pg: 100.
11. Weinhold G (2002) Die Zinnerz-Lagerstätte Altenberg/Osterzgebirge. Bergbaumonographie Band 9, Freiberg. Pg: 283.
12. Lausch H (2024) (Editor) Geologie und Mineralien des Zwitterstocks zu Altenberg. Manuskripte zum Montanwesen um Altenberg und Zinnwald, Bergbaumuseum und Knappenverein Altenberg e.V. Heft 7/2024. Pg: 213.
13. Lahl B (2012) Königliche Topase vom Schneckenstein. *Chemnitzer Verlag*. Pg: 142.
14. Spivak AV, Setkova TV, Borovikova EY, Kvas PS, Balitsky VS, et al. (2021) Physical chemical properties of geomaterials. *Experiment in Geosciences* 27: 105-107.
15. Setkova TV, Balitsky VS, Spivak AV, Kuzmin AV, Borovikova EY, et al. (2024) Crystal growth, composition, structure, and Raman spectroscopy of novel Ga,Ge-rich topaz. *Journal of Crystal Growth* 637-638: 1-10 inclusive, the Supporting Information: 1-18.
16. Xie X, Gu X, Chen M (2023) The discovery of TiO_2-II, the a-PbO_2-structured high-pressure polymorph of rutile, in the Suizhou L6 chondrite. *Acta Geochim* 42: 1-8.
17. Thomas R (2025) The change from the supercritical fluid-melt system into the under-critical stage: The Zinnwald example. *Geol Earth Mar Sci* 7: 1-9.
18. Beny JM, Piriou B (1987) Vibrational spectra of single-crystal topaz. *Phys Chem Minerals* 15: 148-154.
19. Thomas R (2026b) Ultrahigh-pressure and -temperature mineral inclusions in more crustal mineralizations: The role of supercritical fluids. *Geol Earth Mar Sci* 5: 1-2.
20. Thomas R (2024a) The $CaCl_2$-to-rutile phase transition in SnO_2 from high to low pressure in nature. *Geol Earth Mar Sci* 6: 1-4.
21. Thomas R (2024b) Rhomboedric cassiterite as inclusions in tetragonal cassiterite from Slavkovský les – North Bohemia (Czech Republic). *Geol Earth Mar Sci* 6: 1-6.
22. Thomas R, Recknagel U (2024) Lonsdaleite, diamond, and graphite in a lamprophyre: Minette from East-Thuringia/Germany. *Geol Earth Mar Sci* 6: 1-4.
23. Thomas R, Trinkler M (2024) Monocrystalline lonsdaleite in REE-rich fluorite from Sadisdorf and Zinnwald/E-Erzgebirge, Germany. *Geol Earth Mar Sci* 6: 1-5.

24. Thomas R, Davidson P, Rericha A, Recknagel U (2022) Discovery of stishovite in the prismatine-bearing granulite from Waldheim, Germany: A possible role of supercritical fluids of ultrahigh-pressure origin. *Geosciences* 12: 196: 1-13.

25. Thomas R, Rericha A (2025) Extreme element enrichment by the interaction of supercritical fluids from the mantle with crustal rocks. *Minerals* 33: 1-10.

26. Thomas R, Brümmer G, Scheiblauer K (2025) Paradigm change of pegmatite formation – Where does the water come from?

27. Thomas R, Davidson P (2013) The missing link between granites and granitic pegmatites. *Journal of Geosciences* 58: 183-200.

Citation:

Thomas R (2026) Diamond in Pycnite-Rock from Altenberg and in the Topaz from the Famous Schneckenstein Deposit. *Geol Earth Mar Sci* Volume 8(5): 1-7.